

Evaluation of nano-technology-modified zirconia oral implants: a study in rabbits

Lee J, Sieweke JH, Rodriguez NA, Schüpbach P, Lindström H, Susin C, Wikesjö UM. Evaluation of nano-technology-modified zirconia oral implants: a study in rabbits. *J Clin Periodontol* 2009; 36: 610–617. doi: 10.1111/j.1600-051X.2009.01423.x.

Abstract

Objective: The objective of this study was to screen candidate nano-technology-modified, micro-structured zirconia implant surfaces relative to local bone formation and osseointegration.

Materials and Methods: Proprietary nano-technology surface-modified (calcium phosphate: CaP) micro-structured zirconia implants (A and C), control micro-structured zirconia implants (ZiUnite™), and titanium porous oxide implants (TiUnite™) were implanted into the femoral condyle in 40 adult male New Zealand White rabbits. Each animal received one implant in each hind leg; thus, 20 animals received A and C implants and 20 animals received ZiUnite™ and TiUnite™ implants in contralateral hind legs. Ten animals/group were euthanized at weeks 3 and 6 when biopsies of the implant sites were processed for histometric analysis using digital photomicrographs produced using backscatter scanning electron microscopy.

Results: The TiUnite™ surface demonstrated significantly greater bone–implant contact (BIC) ($77.6 \pm 2.6\%$) compared with the A ($64.6 \pm 3.6\%$) and C ($62.2 \pm 3.1\%$) surfaces at 3 weeks ($p < 0.05$). Numerical differences between ZiUnite™ ($70.5 \pm 3.1\%$) and A and C surfaces did not reach statistical significance ($p > 0.05$). Similarly, there were non-significant differences between the TiUnite™ and the ZiUnite™ surfaces ($p > 0.05$). At 6 weeks, there were no significant differences in BIC between the TiUnite™ ($67.1 \pm 4.2\%$), ZiUnite™ ($69.7 \pm 5.7\%$), A ($68.6 \pm 1.9\%$), and C ($64.5 \pm 4.1\%$) surfaces ($p > 0.05$).

Conclusion: TiUnite™ and ZiUnite™ implant surfaces exhibit high levels of osseointegration that, in this model, confirm their advanced osteoconductive properties. Addition of CaP nano-technology to the ZiUnite™ surface does not enhance the already advanced osteoconductivity displayed by the TiUnite™ and ZiUnite™ implant surfaces.

Jaebum Lee¹, Janet H. Sieweke², Nancy A. Rodriguez³, Peter Schüpbach⁴, Håkan Lindström⁵, Cristiano Susin¹ and Ulf M. E. Wikesjö¹

¹Laboratory for Applied Periodontal & Craniofacial Regeneration, Departments of Periodontics & Oral Biology; and

²Department of Periodontics, Medical College of Georgia School of Dentistry, Augusta, GA, USA; ³Laboratory Animal Services, Medical College of Georgia, Augusta, GA, USA; ⁴Peter Schupbach Ltd., Horgen, Switzerland; ⁵Product Development, Nobel Biocare AB, Göteborg, Sweden

Key words: backscatter scanning electron microscopy; bone density; bone–implant contact; calcium phosphate; nano-technology; osseointegration; TiUnite™; ZiUnite™

Accepted for publication 29 March 2009

Endosseous oral implants have become increasingly important in the prosthetic rehabilitation of patients following tooth loss to address aesthetic and functional

Conflict of interest and source of funding statement

This study was supported by a grant from Nobel Biocare AB, Göteborg, Sweden. Håkan Lindström is an employee of Nobel Biocare AB. Ulf ME Wikesjö serves as consultant to Nobel Biocare AB.

demands. The implants need to be placed and become integrated into alveolar bone to become successful prosthetic anchors. The osteoconductivity of the bone anchoring implant surface plays an important role in successful osseointegration. A rabbit long-bone model (Johansson & Albrektsson 1987, Sennerby et al. 2005, Susin et al. 2008) has been used as a valuable screening instrument to select favourable implant surface characteristics/

technologies before pivotal evaluation of actual implant prototypes in large animal models and in patients.

The success of endosseous oral implants is critically related to their osseointegration. Near-immediate bone apposition onto the implant surface appears to be important for desirable early loading strategies. Thus, implant surface properties including topography, composition, and geometry seem decisive for the short- and long-term success of

endosseous oral implants (Le Guehenec et al. 2007). Recent advances have contributed micro- and macro-porous titanium oxide implant surfaces (Hall & Lausmaa 2000, Albrektsson & Wennerberg 2004a, b). Other surface advances include implant surface coating with ceramic products in particular calcium phosphate (CaP)-based technologies (Lacefield et al. 1999, Webster et al. 2000, Xiropaidis et al. 2005). Still other advances have applied nano-technology (Le Guehenec et al. 2007, Coelho et al. 2008, Meirelles et al. 2008a, b) and biotechnology to implant surfaces (Liu et al. 2005, Becker et al. 2006, Hall et al. 2007).

Patient demands for highly aesthetic prosthetic rehabilitation have not only resulted in the use of biotechnology to augment the alveolar bone (for a review, see Wikesjö et al. 2007) but also includes alternative directions in the use of implant base materials. In the cervical area, the colour of a titanium implant might be reflected through and darken the pinkish hue of the gingiva, especially in the presence of a thin gingival biotype. To overcome such cervical discolouration, zirconia is being evaluated as an alternative base material for endosseous oral implants. Zirconia has adequate biocompatibility and mechanical strength (Kohal et al. 2004, Sennerby et al. 2005, Quan et al. 2008). Zirconia implant surface modifications have not been extensively reported. The objective of this study was to screen candidate nano-technology zirconia implant surfaces relative to local bone formation and osseointegration, i.e., implant osteoconductivity.

Materials and Methods

Animals

Forty, adult (>10 months old), male New Zealand White rabbits, weight 5.0–5.5 kg, obtained from a USDA-licensed vendor were used following a protocol approved for this study by the Medical College of Georgia Institutional Animal Care and Use Committee. The animals were routinely inspected and acclimatized before initiation of the surgical protocol. The animals were identified by an ear tag showing animal ID. They were individually housed in stainless-steel cages labelled with cards identifying the study number, species/strain, sex, cage number, and animal ID. The cages were housed in purpose-designed rooms

air-conditioned with 10–20 air-changes/h. Temperature and relative humidity, monitored daily, were $22 \pm 3^\circ\text{C}$ and 50–60%. A 12/12 h light/dark cycle was applied. The animals had ad libitum access to water and a standard laboratory diet throughout the study.

Oral implants

All zirconia ceramic implants exhibited a proprietary porous surface modification in the micrometre scale (ZiUnite™, $\text{Ø}3.75 \times 7$ mm; Nobel Biocare AB, Göteborg, Sweden). Implants in the two test groups, A and C, were further modified by means of two different nano-technologies, each applying the implants with a CaP nano-layer. The control groups included ZiUnite™ implants without the CaP nano-layer and standard micro-structured titanium porous oxide implants (TiUnite™, $\text{Ø}3.75 \times 7$ mm; Nobel Biocare AB) (Fig. 1). R_a

estimates supplied by the manufacturer were $1.0 \mu\text{m}$ for the ZiUnite™ and modified (A and C) ZiUnite™ surfaces, and $1.3 \mu\text{m}$ for the TiUnite™ surface.

The TiUnite™ implant is a commercially pure titanium implant where the naturally occurring oxide layer has been considerably increased by means of anodic oxidation (Hall & Lausmaa 2000). During this process, the oxide layer is not only increased in thickness but also develops a porous structure. Anodic oxidation is a well-known electrochemical process where the implant acts as an anode in an electro-chemical cell, i.e. it is dipped into an acidic electrolyte and a controlled current is allowed to circulate via the anode/implant through the electrolyte to the cathode.

The ZiUnite™ implant is produced by spraying a slurry including zirconia and a pore-forming material onto a pre-shaped zirconia ceramic implant. The

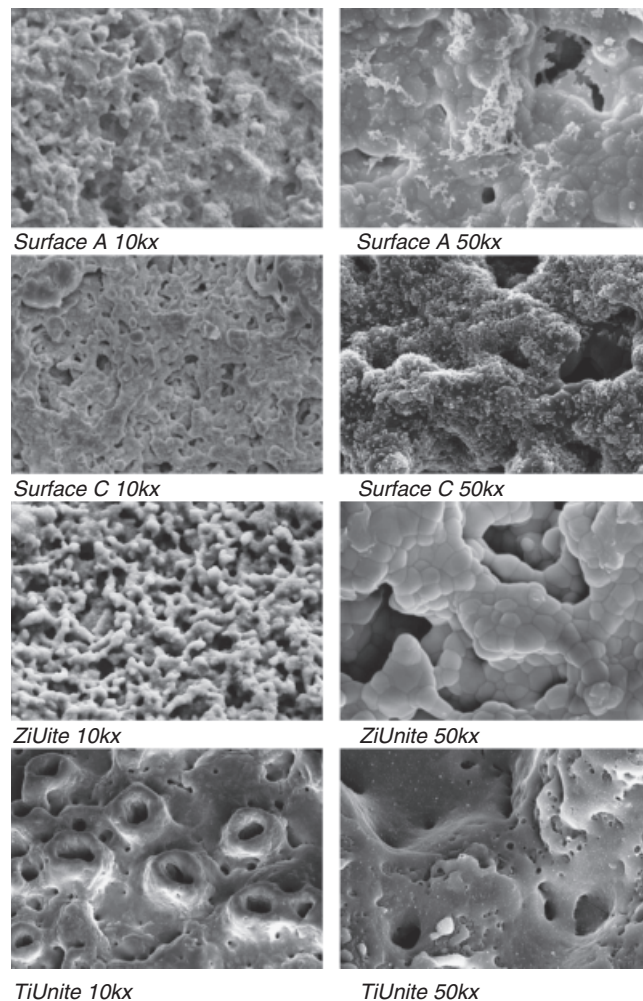


Fig. 1. Scanning electron microscopy photomicrographs of the calcium phosphate-modified (A and C), ZiUnite™, and TiUnite™ implant surfaces.



Fig. 2. Surgical incision (left), implant placement into femoral condyle (left centre), fascia and skin sutured in layers (right centre), and wound closure (right).

slurry is allowed to dry onto the implant surface and is then sintered in an oven to full density, transforming the slurry into a surface coating. During the sintering process, the pore-forming material is burnt away, leaving pores in the coating. Thus, a porous coating of controlled thickness and pore size distribution is sintered onto the core material, resulting in a virtually seamless integration between bulk and coating.

Test implant surface A is produced by immersing the ZiUnite™ implant into a phosphorous-rich solution, followed by immersion into a calcium-rich solution at an elevated temperature, during which a coating with a Ca/P ratio of 1.67 is formed onto the ZiUnite™ implant surface. Following this procedure, the implant is rinsed in clean water and dried at 37°C. The thickness of the A surface was <50 nm.

Implant surface C is produced by applying droplets to the ZiUnite™ implant of a stable solution containing surfactants, water, organic solvent, and crystalline hydroxyapatite nano-particles with a Ca/P ratio of 1.67 (Kjellin & Andersson 2006). The diameter of the hydroxyapatite particles approximates 10 nm. After applying the solution, the implants are dried for 30 min in air, allowing the solvent to evaporate. This is followed by heat treatment at 700°C for 5 min in an oxygen atmosphere to remove all dispersing agents. The thickness of the C surface was <200 nm.

Surgical preparation and experimental procedures

Surgeries were performed using aseptic routines by one experienced surgeon (N. A. R.). General anaesthesia was induced using ketamine/xylazine (45; 5 mg/kg; i.m.). Atropine (0.2 mg/kg; i.m.) was administered to treat for bradycardia and decrease salivary secretion. The animals were intubated with an appropriately sized endotracheal tube or via use of a facemask and placed on iso-

flurane 2–3% for maintenance. The experimental sites were shaved, after which the animals were brought to the operating theatre and the surgical areas were isolated with drapes and disinfected using a 4% chlorhexidine gluconate surgical scrub solution (BD E-Z Scrub; Becton, Dickinson and Company, Franklin Lakes, NJ, USA). Routine lidocaine infiltration anaesthesia (lidocaine 2%, epinephrine 1:100,000, 0.5–1 ml/site) was used at the hind limb experimental sites and the sites were accessed using incisions through the skin and fascia. The bone surfaces were exposed using an elevator. Implants were placed following site preparation using sterile saline-cooled 2.0- and 3.0-mm twist drills, followed by a screw tap. One implant was placed into each (left/right) femoral condyle; implant placement did not interfere with the animal's movement (Fig. 2).

Twenty animals received implants A and C in contralateral femoral sites and twenty animals received ZiUnite™ and TiUnite™ implants for a 3- and 6-week healing interval encompassing ten animals/group/healing interval. A *versus* C, and ZiUnite™ *versus* TiUnite™ implants were alternated between left and right hind limbs.

Fascia and skin were closed in layers using resorbable (Vicryl Rapide 5.0; Ethicon Inc., Somerville, NY, USA) and non-resorbable (GORE-TEX™ Suture CV5, W.L. Gore & Associates Inc., Flagstaff, AZ, USA) sutures and interrupted single and mattress suture techniques as appropriate. The depth of anaesthesia was monitored by observing the response to toe pinch, corneal reflex, and the depth of respiration. The animals received a slow constant rate infusion of lactated Ringer's solution (10–20 ml/kg/h; i.v.) to maintain hydration during surgery.

Post-surgery procedures

A long-acting opioid (buprenorphine HCl, 0.05 mg/kg, i.m., b.i.d./3 days) was administered for pain control. A

broad-spectrum antibiotic (enrofloxacin; 5 mg/kg, i.m./SQ b.i.d./7 days) was administered for infection control. As needed, sutures were removed under sedation (buprenorphine HCl 0.02 mg/kg, acepromazine 0.5 mg/kg i.m.) at approximately 10 days; alternatively, mild manual restraint was used.

Euthanasia

The animals were sedated and euthanized at 3 and 6 weeks post-surgery using an overdose of sodium pentobarbital (100 mg/kg) when tissue specimens including implants and surrounding bone were collected and fixated in a 10% buffered formalin solution for histotechnical preparation.

Histotechnical preparation

The femoral implants (2 implants/animal × 40 animals = 80 implants) were prepared for histologic analysis. The fixated specimens were dehydrated in a graded ethanol series using a dehydration system with agitation and vacuum and embedded in light-curing methacrylate (Technovit 7200 VCL, Kulzer, Wehrheim, Germany). The implants were cut in a mid-axial coronal-apical plane using the sawing-and-grinding technique (EXAKT Apparatebau, Norderstedt, Germany) (Donath & Breuner 1982).

Backscatter scanning electron microscopy

For backscatter scanning electron microscopy, the slices with the ground sections were mounted on special alumina stubs with a silver-containing glue (Plano GmbH, Wetzlar, Germany). The specimens were coated using a 6 nm thick carbon layer using a sputter device (Bal-Tec AG, Balzers, Liechtenstein). Eventually, the alumina stubs were connected to the carbon layer by two thin spurs of a silver-containing glue; this was done to avoid electric loading of the

specimen, which would have disturbed their evaluation. The specimens were evaluated using a Zeiss Supra 40VP scanning electron microscope (Carl Zeiss NTS GmbH, Oberkochen, Germany) using the backscatter detector. Evaluation was performed at 20kV and a working distance of 9 mm (Boyd & Wolfe 2000, Schüpbach et al. 2005).

Histometric analysis

One masked, calibrated examiner (J. L.) performed the histometric analysis using a PC-based image analysis system (Image-Pro Plus™, Media Cybernetic, Silver Spring, MD, USA). The most central section from each implant was used for the analysis. The following parameters were recorded for each implant (Fig. 3):

- *Bone density outside the threads* (BD_{OT}): ratio bone/marrow spaces in the adjoining bone immediately outside the implant threads;
- *Bone density within the threads* (BD_{WT}): ratio bone/marrow spaces in the adjoining bone within the implant threads; and
- *Osseointegration*: percent bone-implant contact (BIC) measured within the area of trabecular (femur) resident bone.

Statistical analysis

Examiner reliability for the histometric evaluation was assessed using the Con-

cordance Correlation Coefficient (Lin 1989, 2000). This coefficient ranges between 0 and 1; the higher the coefficient the greater the reliability. The concordance correlation coefficient for the histometric measurements ranged from 0.95 to 0.98, demonstrating high reliability for all the parameters assessed.

The statistical analysis was performed using Stata 9.2 for Windows (Stata Corporation, College Station, TX, USA). Linear models were used to compare the experimental groups. Clustering of observations within animals was accounted for using appropriated variance estimators. Significance was set at 5% and *p*-values were adjusted for multiple comparisons. Means and standard errors (SE) are presented.

Results

Clinical observations

There were no noteworthy differences in stability between the implants at placement. Most animals/experimental sites exhibited uneventful healing over the 3- and 6-week interval. Four animals were excluded from the study due to various reasons: immediate post-surgery death (1), wound failure exposing implants (2), broken ankle (1), and extensive seroma formation (1). The removed animals were replaced accordingly.

Backscatter scanning electron microscopy observations

All implants showed bone formation directly onto the implant surfaces (Figs 4 and 5). There were no remarkable differences between implants and sites. Two specimens were excluded from the histometric analysis due to defects (fractured bone-implant interface) in the histotechnical preparation. Sites that do not represent a model of trabecular bone well were also excluded from the analysis; our laboratory uses a cut-off BD_{OT} value $>75\%$ to identify such sites. The histotechnical preparation of some specimens prevented meaningful evaluation of BD_{OT} and on one occasion BD_{WT} .

Histometric analysis

The results of the histometric analysis for the 3-week specimens are shown in Table 1. Following a 3-week healing interval, the TiUnite™ surface demonstrated a significantly greater BIC ($77.6 \pm 2.6\%$) compared with that of the nano-technology-structured implant surfaces A ($64.6 \pm 3.6\%$) and C ($62.2 \pm 3.1\%$) ($p < 0.05$). There were no significant differences in mean BD_{OT} and BD_{WT} between the TiUnite™ ($48.9 \pm 1.5\%$ and $40.5 \pm 1.7\%$), the A ($47.7 \pm 4.2\%$ and $34.3 \pm 3.2\%$), and C ($48.5 \pm 1.5\%$ and $39.6 \pm 3.5\%$) implant surfaces at the 3-week healing interval ($p > 0.05$). Numerical differences in BIC between the ZiUnite™ ($70.5 \pm 3.1\%$) and the A and C implant surfaces did not reach statistical significance ($p > 0.05$), although significant differences in BD_{OT} and BD_{WT} were observed ($p < 0.05$). Similarly, there were non-significant differences in BIC between the TiUnite™ and the ZiUnite™ implant surfaces ($p > 0.05$).

The results of the histometric analysis for the 6-week specimens are shown in Table 2. There were no significant differences in BIC between the TiUnite™ ($67.1 \pm 4.2\%$), ZiUnite™ ($69.7 \pm 5.7\%$), A ($68.6 \pm 1.9\%$), and C ($64.5 \pm 4.1\%$) implant surfaces at the 6-week healing interval ($p > 0.05$). Similarly, there were no statistically significant or meaningful differences in BD_{OT} and BD_{WT} among the various implant surfaces; the mean BD_{OT} ranged from 49.7% to 53.7%, and BD_{WT} from 39.4% to 48.7%.

Discussion

The present study showed a favourable tissue response to CaP nano-technology-

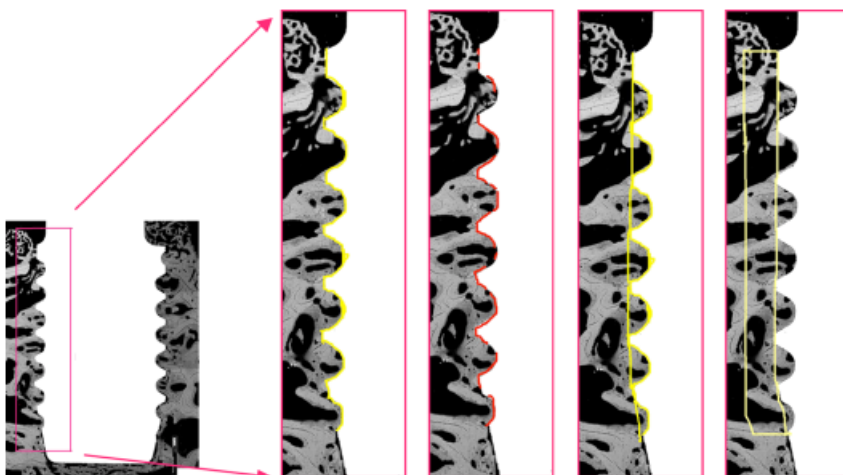


Fig. 3. Schematic representation of the histometric analysis including representative backscatter scanning electron microscopy photomicrograph of a ZiUnite™ implant placed into the femoral condyle. Magnified sections show the implant thread area under analysis (left), the bone-implant contact (BIC) analysis (left centre); the area of interest for the analysis of bone density within the threads (BD_{WT}) (right centre); and the area of interest for the analysis of bone density immediately outside the threads (BD_{OT}) (right).

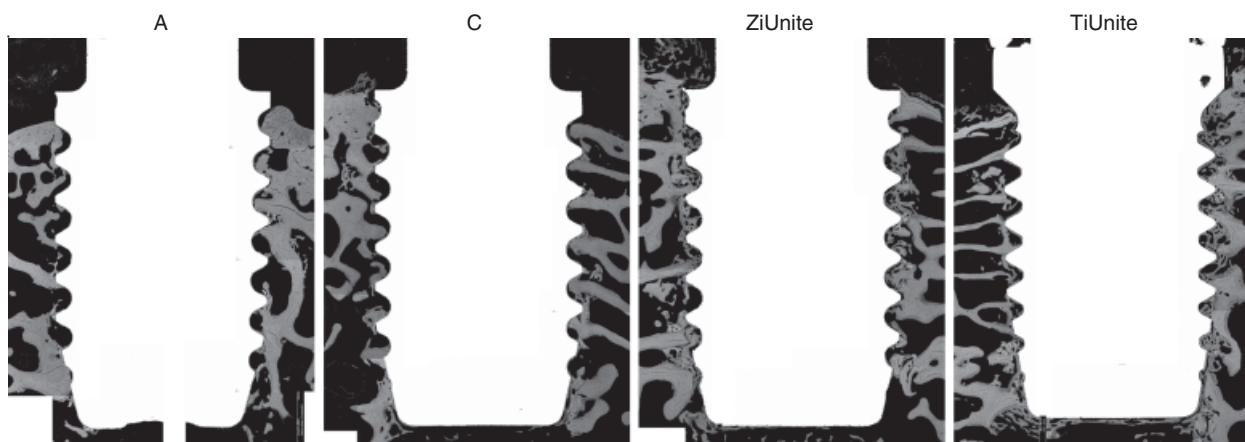


Fig. 4. Backscatter scanning electron microscopy photomicrographs for animals receiving A, C, ZiUnite™, and TiUnite™ endosseous oral implants following a 3-week healing interval.

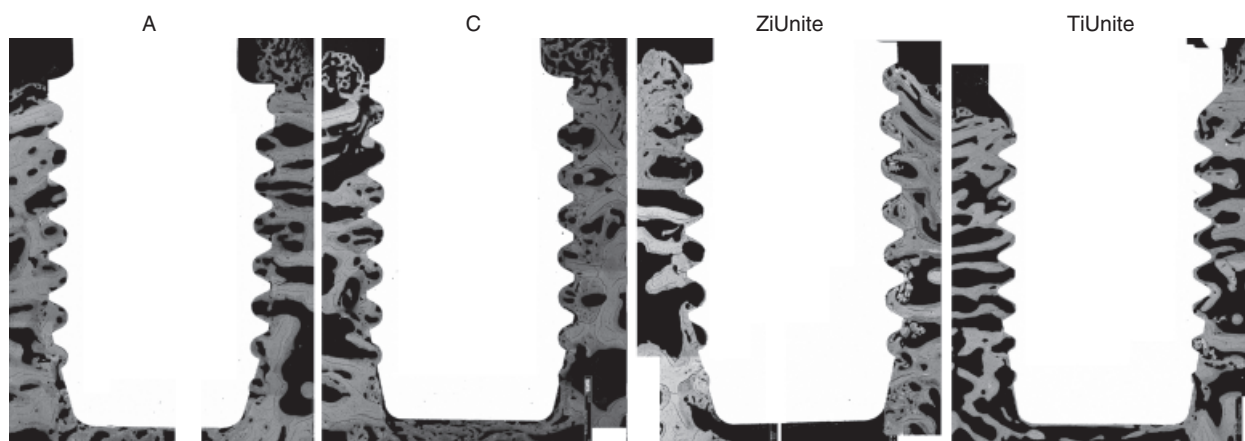


Fig. 5. Backscatter scanning electron microscopy photomicrographs for animals receiving A, C, ZiUnite™, and TiUnite™ endosseous oral implants following a 6-week healing interval.

Table 1. Group means (\pm SE) for the backscatter scanning electron microscopy histometric analysis following a 3-week healing interval

Surface	BD _{OT} (%)	BD _{WT} (%)	BIC (%)
A	47.7 \pm 4.2 A	34.3 \pm 3.2 A	64.6 \pm 3.6 A
C	48.5 \pm 1.5 A	39.6 \pm 3.5 A	62.2 \pm 3.1 A
ZiUnite™	54.7 \pm 2.4 B	45.5 \pm 2.5 B	70.5 \pm 3.1 AB
TiUnite™	48.9 \pm 1.5 A	40.5 \pm 1.7 AB	77.6 \pm 2.6 B

Means followed by the same capital letters do not differ statistically ($p > 0.05$).

BD_{OT}, bone density immediately outside the threads; BD_{WT}, bone density within the threads; BIC: bone-implant contact; SE, standard error.

modified ZiUnite™ as well as to control ZiUnite™ and TiUnite™ implants without dramatic or meaningful differences between the implant surface technologies following 3- and 6-week healing intervals using a rabbit trabecular bone model. The histometric evaluation indicates that all surfaces tested exhibited a high level of osseointegration, suggesting that they might all be osteoconductive, i.e., the implant surfaces enhanced osteogenic bone formation as shown in

various other studies comparing TiUnite™ with control turned titanium implants (Glauser et al. 2001, Rocci et al. 2003). The rabbit femoral trabecular bone model herein is used for its potential to display the osteoconductivity of candidate implant surfaces. Because bone healing in rabbit has been suggested to be two to three times faster than in humans (Robert et al. 1987), healing intervals of 3 and 6 weeks were chosen. The 3-week interval

approximates a healing interval of 6–9 weeks in humans and this interval is suggested for early bone healing following implant placement. The 6-week interval approximates a healing interval of 12–18 weeks in humans suggested to coincide with bone remodelling (LaS-tayo et al. 2003, Matos et al. 2008).

Backscatter scanning electron microscopy is based on compositional contrast and provides information not only on the surface but also within a specimen (Goldstein et al. 1984, Boyde & Wolfe 2000). The present study used backscatter scanning electron microscopy to produce photomicrographs of the zirconia ceramic implants for histometric analysis. The reason for this is twofold. First, processing of ceramic implants using traditional histotechnical cutting-grinding techniques (Donath & Breuner 1982) may not translate well to zirconia ceramic implants to standards demanded for histometric analysis using

Table 2. Group means (\pm SE) for the backscatter scanning electron microscopy histometric analysis following a 6-week healing interval

Surface	BD _{OT} (%)	BD _{WT} (%)	BIC (%)
A	51.8 \pm 3.0 A	45.4 \pm 3.4 AB	68.6 \pm 1.9 A
C	49.7 \pm 1.6 A	39.4 \pm 3.5 A	64.5 \pm 4.1 A
ZiUnite™	51.2 \pm 3.1 A	47.4 \pm 2.3 B	69.7 \pm 5.7 A
TiUnite™	53.7 \pm 1.9 A	48.7 \pm 1.7 B	67.1 \pm 4.2 A

Means followed by the same capital letters do not differ statistically ($p > 0.05$).

BD_{OT}, bone density immediately outside the threads; BD_{WT}, bone density within the threads; BIC, bone-implant contact; SE, standard error.

light microscopy. Second, a parallel study in our laboratory evaluating conventional titanium implants suggested that backscatter scanning electron microscopy produced photomicrographs superior in contrast, and thus more diagnostic, compared with photomicrographs generated from histologic specimens for light microscopy processed using routine histotechnical cutting-grinding techniques (N. Poulos et al. 2009, unpublished data). Consequently, backscatter scanning electron microscopy appears to be an acceptable alternative for histometric analysis of immediate bone density and osseointegration.

The major component for the clinical success of oral implants is the establishment of an immediate contact between the implant and adjoining bone. It is thought that the bone response is influenced by the implant surface texture and composition (Wennerberg 1996, Sul et al. 2004). Moderate surface roughness appears to be associated with increased bone contact (Buser et al. 1991, Shalabi et al. 2006). Thus, various methods including oxidation, sand blasting, and acid etching have been adopted to enhance implant surface texture (Albrektsson & Wennerberg 2004a,b). CaP is regarded as a bioactive material having a direct bonding capacity to surrounding bone (Thomas et al. 1987, Geesink et al. 1988, Tisel et al. 1994, Sul et al. 2004). CaP implant coatings have been used to accelerate early-stage bone formation and osseointegration (Thomas et al. 1987, Geesink et al. 1988, Tisel et al. 1994, Kim et al. 2004a,b, Sul et al. 2004, Quan et al. 2008). Cohesive failure between the implant and a CaP coating has been observed and has been related to implant failure (Buser et al. 1991, Jansen et al. 1993). Recently, developed CaP nano-technology implant coatings have been shown to accelerate local bone formation (Webster et al. 2000, Yang 2001). Significantly increased early bone for-

mation has been observed at hydroxyapatite nano-coated implants compared with control (Meirelles et al. 2008a). This increased local bone formation does not appear to be unique to hydroxyapatite nano-structures as increased bone formation is also observed at titania nano-structures (Meirelles et al. 2008b). The CaP nano-coatings used in this study were thin and dense, retaining the texture of the underlying ZiUnite™ surface. In other words, the CaP nano-coating may not have significantly altered the surface texture but only changed the surface composition of the ZiUnite™ implant.

Zirconia ceramics exhibit favourable mechanical properties and biocompatibility, which make them candidates for oral implants (Piconi & Maccauro 1999, Kohal et al. 2004, Sennerby et al. 2005, Quan et al. 2008). Zirconia surfaces show reduced bacterial colonization compared with titanium (Rimondini et al. 2002, Scarano et al. 2004). Zirconia exhibits colour properties closely related to teeth for optimal aesthetics in patients with thin gingival biotypes, which cannot be met using titanium implants. Several reports have documented successful application of zirconia implants in preclinical (Kohal et al. 2004, Sennerby et al. 2005) and clinical settings (Oliva et al. 2007, Pirker & Kocher 2008). Zirconia implants with micro-structured ZiUnite™ surfaces exhibit enhanced osseointegration compared with smooth surface zirconia implants (Sennerby et al. 2005, Oliva et al. 2007). The candidate CaP nano-technology-structured ZiUnite™ implants showed a somewhat lower, but statistically significant, osseointegration compared with the TiUnite™ implants at 3 weeks although the immediate osseous environment evaluated using bone density assessments did not differ among the surfaces. This observation in itself may depend on differences in chemistry, micro-, or nano-topography between the surfaces evaluated. Moreover, this

observation affirms favourable early bone-implant surface interactions of the TiUnite™ surface observed in various other settings and bone qualities (Zechner et al. 2003, Huang et al. 2005, Xiropaidis et al. 2005). Following a 6-week healing interval, however, the apparent advantage of the TiUnite™ surface was reached by the various ZiUnite™ implants irrespective of surface treatment.

In conclusion, both TiUnite™ and ZiUnite™ implant surfaces exhibit high levels of osseointegration that, in this model, confirm their advanced osteoconductive properties. Addition of CaP nano-technology to the ZiUnite™ surface does not enhance the osteoconductivity displayed by the TiUnite™ and ZiUnite™ implant surfaces.

Acknowledgement

The authors thank Cedrick Bouey and Jamie Frank for animal technical care and husbandry, and Kimberly Curtis for administrative support.

References

- Albrektsson, T. & Wennerberg, A. (2004a) Oral implant surfaces: part 1 – review focusing on topographic and chemical properties of different surfaces and in vivo responses to them. *The International Journal of Prosthodontics* **17**, 536–543.
- Albrektsson, T. & Wennerberg, A. (2004b) Oral implant surfaces: part 2 – review focusing on clinical knowledge of different surfaces. *The International Journal of Prosthodontics* **17**, 544–564.
- Becker, J., Kirsch, A., Schwarz, F., Chatzinikolaïdou, M., Rothamel, D., Lekovic, V., Laub, M. & Jennissen, H. P. (2006) Bone apposition to titanium implants bio-coated with recombinant human bone morphogenetic protein-2 (rhBMP-2). A pilot study in dogs. *Clinical Oral Investigations* **10**, 217–224.
- Boyde, A. & Wolfe, L. A. (2000) Spatial and temporal patterns of bone growth around endosseous implants: a critical study of microscopic methods. In: Davies, J. E. (ed). *Bone Engineering*, pp. 321–331. Toronto, Canada: em squared Inc.
- Buser, D., Schenk, R. K., Steinemann, S., Fiorellini, J. P., Fox, C. H. & Stich, H. (1991) Influence of surface characteristics on bone integration of titanium implants. A histomorphometric study in miniature pigs. *Journal of Biomedical Materials Research* **25**, 889–902.
- Coelho, P. G., Cardaropoli, G., Suzuki, M. & Lemons, J. E. (2008) Early healing of nanothickness bioceramic coatings on dental

- implants. An experimental study in dogs. *Journal of Biomedical Materials Research. Part B, Applied Biomaterials* **88**, 387–393. [Epub ahead of print].
- Donath, K. & Breuner, G. (1982) A method for the study of undecalcified bones and teeth with attached soft tissues. The Sage–Schliff (sawing and grinding) technique. *Journal of Oral Pathology* **11**, 318–326.
- Geesink, R. G. T., Groot, K. D. & Klein, C. P. A. T. (1988) Bonding of bone to apatite-coated implants. *The Journal of Bone and Joint Surgery. British Volume* **70-B**, 17–22.
- Glauser, R., Portmann, M., Ruhsteller, P., Lundgren, A. K., Hämmerle, C. H. F. & Gottlow, J. (2001) Stability measurements of immediately loaded machined and oxidized implants in the posterior maxilla, a comparative clinical study using resonance frequency analysis. *Applied Osseointegration Research* **2**, 27–29.
- Goldstein, J. I., Newbury, D. E., Echlin, P., Joy, D. C., Fiori, C. & Lifshin, E. (1984) *Scanning Electron Microscopy and X-Ray Microanalysis; A Text for Biologists, Material Science, and Geologists*, 2nd edition. New York: Plenum Press.
- Hall, J. & Lausmaa, J. (2000) Properties of a new porous oxide surface on titanium implants. *Applied Osseointegration Research* **1**, 5–8.
- Hall, J., Sorensen, R. G., Wozney, J. M. & Wikesjö, U. M. E. (2007) Bone formation at rhBMP-2-coated titanium implants in the rat ectopic model. *Journal of Clinical Periodontology* **34**, 444–451.
- Huang, Y. H., Xiropaidis, A. V., Sorensen, R. G., Albandar, J. M., Hall, J. & Wikesjö, U. M. E. (2005) Bone formation at titanium porous oxide (TiUnite) oral implants in type IV bone. *Clinical Oral Implants Research* **16**, 105–111.
- Jansen, J. A., van der Waerden, J. P. C. M. & Wolke, J. G. C. (1993) Histologic investigation of the biologic behavior of different hydroxyapatite plasma-sprayed coatings in rabbits. *Journal of Biomedical Materials Research* **27**, 603–610.
- Johansson, C. & Albrektsson, T. (1987) Integration of screw implants in the rabbit: a 1-year follow-up of removal torque of titanium implants. *The International Journal of Oral and Maxillofacial Implants* **2**, 69–75.
- Kim, H. M., Kim, H. E. & Knowles, J. C. (2004a) Hard-tissue-engineered zirconia porous scaffolds with hydroxyapatite sol–gel and slurry coatings. *Journal of Biomedical Materials Research* **70B**, 270–277.
- Kim, H. M., Kim, H. E., Salihi, V. & Knowles, J. C. (2004b) Dissolution control and cellular responses of calcium phosphate coatings on zirconia porous scaffold. *Journal of Biomedical Materials Research* **68A**, 522–530.
- Kjellin, P. & Andersson, M. (2006) SE-0401524-4, assignee. Synthetic nano-sized crystalline calcium phosphate and method of production, Patent SE527610, 25 April 2006.
- Kohal, R. J., Weng, D., Bächle, M. & Strub, J. R. (2004) Loaded custom-made zirconia and titanium implants show similar osseointegration: an animal experiment. *Journal of Periodontology* **75**, 1262–1268.
- Lacefield, W. R. (1999) Materials characteristics of uncoated/ceramic-coated implant materials. *Advances in Dental Research* **13**, 21–26.
- LaStayo, P. C., Winters, K. M. & Hardy, M. (2003) Fracture healing: bone healing, fracture management, and current concepts related to the hand. *Journal of Hand Therapy* **16**, 81–93.
- Le Guehennec, L., Soueiden, A., Layrolle, P. & Amouriq, Y. (2007) Surface treatments of titanium dental implants for rapid osseointegration. *Dental Materials* **23**, 844–854.
- Lin, L. I.-K. (1989) A concordance correlation coefficient to evaluate reproducibility. *Biometrics* **45**, 255–268.
- Lin, L. I.-K. (2000) A note on the concordance correlation coefficient. *Biometrics* **56**, 324–325.
- Liu, Y., de Groot, K. & Hunziker, E. B. (2005) BMP-2 liberated from biomimetic implant coatings induces and sustains direct ossification in an ectopic rat model. *Bone* **36**, 745–757.
- Matos, M. A., Araújo, F. P. & Paixão, F. B. (2008) Histomorphometric evaluation of bone healing in rabbit fibular osteotomy model without fixation. *Journal of Orthopedic Surgery and Research* **3**, 1749–1799.
- Meirelles, L., Arvidsson, A., Andersson, M., Kjellin, P., Albrektsson, T. & Wennerberg, A. (2008a) Nanohydroxyapatite structures influence early bone formation. *Journal of Biomedical Materials Research. Part A* **87**, 299–307.
- Meirelles, L., Melin, L., Peltola, T., Kjellin, P., Kangasniemi, I., Currie, F., Andersson, M., Albrektsson, T. & Wennerberg, A. (2008b) Effect of hydroxyapatite and titania nanostructures on early in vivo bone response. *Clinical Oral Implants Research* **10**, 245–254.
- Oliva, J., Oliva, X. & Oliva, J. D. (2007) One-year follow-up of first consecutive 100 zirconia dental implants in humans: a comparison of 2 different rough surfaces. *The International Journal of Oral and Maxillofacial Implants* **22**, 430–435.
- Piconi, C. & Maccauro, G. (1999) Zirconia as a ceramic biomaterial. *Biomaterials* **20**, 1–25.
- Pirker, W. & Kocher, A. (2008) Immediate, non-submerged, root-analogue zirconia implant in single tooth replacement. *The International Journal of Maxillofacial Surgery* **37**, 293–295.
- Quan, R., Yang, D., Wu, X., Wang, H., Miao, X. & Li, W. (2008) In vitro and in vivo biocompatibility of graded hydroxyapatite-zirconia composite bioceramic. *Journal of Materials Science. Materials in Medicine* **19**, 183–187.
- Rimondini, L., Cerroni, L., Carrassi, A. & Torricelli, P. (2002) Bacterial colonization of zirconia ceramic surfaces: an in vitro and in vivo study. *The International Journal of Oral and Maxillofacial Implants* **17**, 793–798.
- Robert, W. E., Turly, P. K., Brezniak, N. & Fielder, P. J. (1987) Implant: bone physiology and metabolism. *Journal California Dental Association* **15**, 54–61.
- Rocci, A., Martignoni, M. & Gottlow, J. (2003) Immediate loading of Brånemark System TiUnite and machined-surface implants in the posterior mandible: a randomized open-ended clinical trial. *Clinical Implant Dentistry and Related Research* **5** (Suppl. 1), S57–S63.
- Scarano, A., Piattelli, M., Caputi, S., Favero, G. A. & Piattelli, A. (2004) Bacterial adhesion on commercially pure titanium and zirconium oxide disks: an in vivo human study. *Journal of Periodontology* **75**, 292–296.
- Schüpbach, P., Glauser, R., Rocci, A., Martignoni, M., Sennerby, L., Lundgren, A. & Gottlow, J. (2005) The human bone-oxidized titanium implant interface: a light microscopic, scanning electron microscopic, backscatter scanning electron microscopic, and energy-dispersive x-ray study of clinically retrieved dental implants. *Clinical Implant Dentistry and Related Research* **7** (Suppl. 1), S36–S43.
- Sennerby, L., Dasmah, A., Larsson, B. & Iverhed, M. (2005) Bone tissue responses to surface-modified zirconia implants: a histomorphometric and removal torque study in the rabbit. *Clinical Implant Dentistry and Related Research* **7** (Suppl. 1), S13–S20.
- Shalabi, M. M., Gortemaker, A., van't Hof, M. A., Jansen, J. A. & Creugers, N. H. J. (2006) Implant surface roughness and bone healing: a systematic review. *Journal of Dental Research* **85**, 495–500.
- Sul, Y. T., Byon, E. S. & Jeong, Y. S. (2004) Biomechanical measurements of calcium-incorporated oxidized implants in rabbit bone: effect of calcium surface chemistry of a novel implant. *Clinical Implant Dentistry and Related Research* **6**, 101–110.
- Susin, C., Qahash, M., Hall, J., Sennerby, L. & Wikesjö, U. M. E. (2008) Histological and biomechanical evaluation of phosphorylcholine-coated titanium implants. *Journal of Clinical Periodontology* **35**, 270–275.
- Thomas, K. A., Kay, J. F., Cook, S. D. & Jarcho, M. (1987) The effect of surface macro texture and hydroxyapatite coating on the mechanical strengths and histologic profiles of titanium implant materials. *Journal of Biomedical Material Research* **21**, 1395–1414.
- Tisel, C. L., Goldberg, V. M., Parr, J. A., Bensusan, J. S., Stikoff, L. S. & Stevenson, S. (1994) The influence of a hydroxyapatite and tricalciumphosphate coating on bone growth into titanium fiber–metal implants. *Journal of Bone and Joint Surgery* **76**, 139–171.
- Webster, T. J., Ergun, C., Doremus, R. H., Siegel, R. W. & Bizios, R. (2000) Enhanced functions of osteoblasts on nanophase ceramics. *Biomaterials* **21**, 1803–1810.
- Wennerberg, A. (1996) *On Surface Roughness and Implant Incorporation*. Göteborg, Sweden: Göteborg University.

Wikeshj , U. M. E., Huang, Y. H., Polimeni, G. & Qahash, M. (2007) Bone morphogenetic proteins: a realistic alternative to bone grafting for alveolar reconstruction. *Oral and Maxillofacial Surgery Clinics of North America* **19**, 535–551.

Xiropaidis, A. V., Qahash, M., Lim, W. H., Shanaman, R. H., Rohrer, M. D., Wikeshj , U. M. E. & Hall, J. (2005) Bone–implant contact at calcium phosphate-coated and porous titanium oxide (TiUnite)-modified oral implants.

Clinical Oral Implants Research **16**, 532–539.

Yang, C. (2001) The effect of calcium phosphate implant coating on osteoconduction. *Oral Surgery, Oral Medicine, Oral Pathology, Oral Radiology, and Endodontics* **92**, 606–609.

Zechner, W., Tangl, S., F rst, G., Tepper, G., Thams, U., Mailath, G. & Watzek, G. (2003) Osseous healing characteristics of three different implant types. *Clinical Oral Implants Research* **14**, 150–157.

Address:

Jaebum Lee

Laboratory for Applied Periodontal & Craniofacial Regeneration

Departments of Periodontics & Oral Biology

Medical College of Georgia School of Dentistry

1120 15th Street AD-1432

Augusta

GA 30912

USA

E-mail: Jaelee@mcg.edu

Clinical Relevance

Scientific rationale for the study: The objective of this study was to screen candidate nano-technology-modified, micro-structured zirconia implant surfaces relative to local bone formation and osseointegration.

Principal findings: Using the rabbit femoral trabecular bone model, we show that CaP nano-technology modified zirconia (ZiUnite), ZiUnite, and TiUnite implant surfaces all exhibit high levels of osseointegration.

Practical implications: Addition of CaP nano-technology to the ZiUnite surface does not enhance the already advanced osteoconductivity displayed by the TiUnite and ZiUnite implant surfaces.

This document is a scanned copy of a printed document. No warranty is given about the accuracy of the copy. Users should refer to the original published version of the material.